



Direction-dependent adhesion of water strider's legs for water-walking

Liang Xu^{a,c}, Xi Yao^a, Yongmei Zheng^{b,*}

^a Beijing National Laboratory for Molecular Sciences (BNLMS), Key Laboratory of Organic Solids, Institute of Chemistry, Chinese Academy of Sciences, Beijing 100190, PR China

^b Key Laboratory of Bio-Inspired Smart Interfacial Science and Technology of Ministry of Education, School of Chemistry and Environment, Beihang University, Beijing 100191, PR China

^c Graduate School of Chinese Academy of Sciences, Beijing 100049, PR China

ARTICLE INFO

Article history:

Received 22 May 2012

Accepted 30 May 2012

Available online 8 June 2012

Keywords:

Directional

Adhesion

Water strider

Water-walking

Water repellency

ABSTRACT

We report the direction-dependent adhesion of water strider's legs for fleetly walking on water surface. The flexibly oriented setae of legs involving the hierarchical micro/nanostructure tune effectively the solid–liquid–air three phase interfaces in two opposite directions: the direction along the setae and opposite the setae, generating different adhesion dependent on the direction. A model is proposed to elucidate the underlying mechanism of water-walking based on direction-dependent adhesion induced by the orientation of the aligned setae. This finding will improve our understandings of the interaction between the oriented structured surface and water surface, and is significant to boost biomimetic structured surface that can be applied into microfluidics and aquatic microdevices.

© 2012 Elsevier Masson SAS. All rights reserved.

1. Introduction

Water striders are well-known water-walking insects for their remarkable abilities to freely stand and fleetly walk on water surface, which attracted great attention in foundational and biomimetic researches [1–13]. Recently, Bush et al. gave a reasonable explanation on hydrodynamics of water striders in water surface propulsion and climbing menisci [4–7]. Our previous work proposed that the unique micro/nano-hierarchical structures of the aligned setae with nanoscale grooves on water strider's leg endow it with superior water repellency [8,9]. However, an aspect related to the effect of setae orientation of water strider's leg on the water-walking is still not clear so far. It has been known that the asymmetric patterned structure can induce anisotropic interfacial properties of bio-surfaces responsible for special functions [14–18]. For instance, rice leaf enables droplet roll off along parallel to the direction of leaf edge due to the papillae aligned parallel to the direction of leaf edge [14], and butterfly wing forms directional adhesion to water droplet by means of the oriented arrangement of the stepwise stacked scales on the wing [15]. Inspired by nature, these direction-dependent properties were excellent exhibited on artificial micro-patterned surface consisted of oriented grooves and asymmetric sawteeth rough surface. They could be applied in

microfluidic devices, evaporation-induced pattern formation, and easy-cleaning coatings [19–24].

In this work, we reveal that the orientally aligned setae on the water strider's legs induce direction-dependent adhesion to water at one-dimensional level in two opposite directions: i.e., the directions along the setae (defined as AS direction) and opposite the setae (defined as OS direction). Water droplets roll along leg more easily in AS direction than in OS direction, more obvious adhesion is observed when water droplet slides along the leg in OS direction, as well as larger resistance exists when the leg is immersed in water in OS direction. A model is proposed to explain the underlying mechanism of direction-dependent adhesion induced by the orientation of the aligned setae. According to the experimental results, a reasonable elucidation on the assistant role of oriented-structure-induced adhesion in water strider's effortless surface standing and moving is provided. The investigation will offer an insight into the propulsion of water-walking via the superhydrophobic oriented structured surface, and is significant to boost the novel biomimetic structured surface design that can be applied into microfluidics and aquatic microdevices [21,23,25].

2. Experimental

2.1. Preparation of sample

The water striders specimens' weight is about 10 mg and the middle/hind legs of which were about 20 mm long. To study the

* Corresponding author.

E-mail address: zhengym@buaa.edu.cn (Y. Zheng).

structured morphology and wetting properties, water strider's legs were carefully selected and cleaned through blowing with nitrogen gas. All the samples were taken from living water strider just before the experiments in order to keep the freshness and real performance.

2.2. Characterization of microstructure

The structured morphology of water strider's leg was observed under a field-emission scanning electron microscope (FE-SEM, JSM-6700F, Japan) and an environmental scanning electron microscope (ESEM, Hitachi S-3000N, Japan).

2.3. Measurement of the directional rolling angle

The wetting properties of water strider's leg were measured using a contact angle meter system (OCA20, Dataphysics, Germany). In order to test the directional water repellency of the legs, eight well-chosen legs with diameters of about 220 μm were close packed and fixed on a glass slide to form a plane surface, with the setae of which inclining to the same orientation. Subsequently, the sample of the as-prepared close-packed-leg surface was placed on the tilting board, so distinct rolling angles of water droplet (3 μL) on the sample in the AS or OS direction could be observed. Meanwhile, a high speed CCD camera was used to monitor rolling behaviors of the water droplet during the measurements.

2.4. Adhesive behaviors of a droplet sliding along leg

A 5 μL water droplet was hung on a syringe needle, and then it was controlled to slide along a single water strider's leg back and forth. Adhesive behaviors between water droplet and leg in different sliding directions were observed and recorded by a CCD camera.

2.5. Immersion experiments

To explore the interactions between water and water strider's leg with different setae orientation, an immersion experiment was designed using a high-sensitivity microelectronic balance system (DCAT 20, Dataphysics, Germany). At first, a well-chosen straight part of water strider's leg was vertically suspended on the sample holder of the balance, and the force of the balance was initialized to zero. Then, a water vessel placed below the sample was lifted upwards to the leg at a constant speed of 0.1 mm/s, so the leg was gradually immersed in water up to a given depth of 5 mm. During the immersion process, the force–depth curves were automatically recorded by the microelectronic balance system. Deionized water was used in all the tests, which were carried out at the ambient temperature of 20 $^{\circ}\text{C}$.

3. Results and discussion

To reveal the direction-dependent properties, the details of microstructure of water strider's legs are firstly observed by SEM. As shown in Fig. 1, numerous aligned chitinous setae exist on the leg, with many regular elaborate nanoscale grooves. Most of tiny setae are $\sim 50\text{ }\mu\text{m}$ in length and $\sim 2\text{ }\mu\text{m}$ in diameter, with the distance of $\sim 10\text{ }\mu\text{m}$ between adjacent setae. All the aligned setae orientally incline to the direction of leg tip, with an inclination angle θ of about 25° to leg surface. The solid–liquid contact ways can modulate the contour, length, and continuity of the solid–air–liquid three-phase contact line (TCL), which could impact the contact angle hysteresis, rolling angle and surface adhesion [26,27]. For the aligned setae orientally inclined, similar

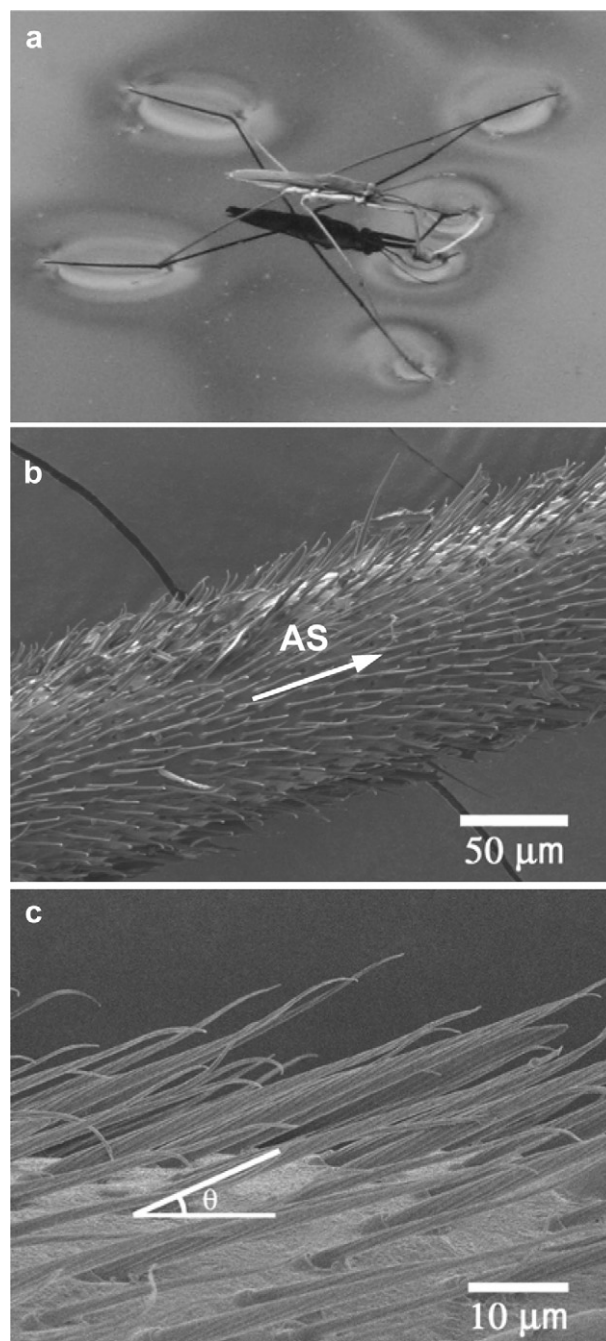


Fig. 1. SEM images, oriented morphology of water strider's leg. (a) A living water strider stands on water surface. (b) Aligned setae on a water strider's leg incline orientally, and the arrow denotes the orientation of the aligned setae (i.e., AS direction). (c) Aligned setae with an inclination angle of θ to leg surface.

to the stepwise stacked scales on butterfly wings, the solid–liquid contact ways could be tuned by the setae orientation, so water droplets on such an oriented structured surface may display directional adhesion at one-dimensional level. Conventionally, rolling behavior of a water droplet on surface reflects the surface adhesion with water, so a water droplet is used to act on the leg to measure the rolling angle. However, a water droplet could not stay on a single cylindric leg steadily and easily rolls off, due to the superhydrophobicity of the surface and less water contact area. The observed result shows that the rolling angles of water droplet vary little in the AS or OS direction, with a difference less than 1° , which demonstrates no distinctly different adhesion on water strider's leg

with the setae orientation by such a conventional experiment method. Thus, a close-packed-leg surface of eight legs oriented in the same direction is prepared to enlarge the contact area with water droplet acted on the leg for further investigation.

Considering that water strider is residing on water surface, and allows its legs contact with water surface for long meanwhile acted by water pressure in rowing, we simply simulate the living condition of water strider's legs on water surface to ensure sufficient contact with water. That is, a pressing force exerted on the water droplet contacts with the close-packed-leg surface so as to enhance the interaction between water droplet and the micro setae (Fig. 2). Firstly, a superhydrophobic polytetrafluoroethylene (PTFE) plate was hung horizontally over water droplet on the close-packed-leg surface, then the plate was controlled to press water droplet, with the pressure of about 120 Pa calculated by Laplace equation [28]. Finally, the plate was removed to withdraw the pressure, and the water static contact angle on the close-packed-leg surface decreased (Fig. 2a). After this treatment, rolling angles in two opposite directions were measured again. Fig. 2b showed three representative images taken in the process of a water droplet rolling off leg surface with a gradual tilting. The water droplet would roll off at a tilting angle of $11.1 \pm 1.8^\circ$ in the AS direction, while the water droplet would be pinned at a tilting angle of $18.6 \pm 2.0^\circ$ in the OS direction. It exhibited distinct difference of rolling angles between AS and OS direction, corresponding to different adhesion dependent on the direction, where the water droplet trended to roll off in the AS direction. Compared with the slight difference (less than 1°) in rolling angles before water droplet was pressed, there was a distinct difference (about 7°) in two opposite directions, indicating that the pressure amplified the asymmetry of water droplet rolling behavior. It is understood that a superhydrophobic rough surface in Cassie state could transfer to

Wenzel state or metastable state under pressure, with a decrease in contact angle and an increase in rolling angle [28,29]. For the superior water repellency of water strider's leg, water droplet can only contact the tips of the setae in a Cassie mode but not penetrate into gaps among the setae, with an air cushion beneath it [8]. After pressing, water could get into gaps in rough surface partially to exclude air cushion, meanwhile the TCL moved downwards from the tips along the side-surface of the setae [9,26,27]. In this case, the TCL was pinned on side-surface of the setae, where the orientation of setae confined the rolling behaviors of water droplet. So the distinct direction-dependent adhesion emerged with the aid of pressure.

Furthermore, adhesive behaviors to a water droplet sliding on a single strider leg were investigated. A 5 μL water droplet hung a syringe needle was controlled to slide along a single leg back and forth, and distinctly different adhesive behaviors were observed in the AS and OS directions. As shown in Fig. 3, when a water droplet slid in the OS direction (Fig. 3a–d), some adhesion happened between water and setae, which extended the contact with setae, accompanying with the increasing inclination angle. While in the AS direction (Fig. 3e–h), no apparent adhesion can be observed and the water droplet suspended onto setae in a typical Cassie's mode, accompanying with discontinuous TCL, meanwhile, the setae slightly decreased its inclination angle (the insets of Fig. 3f and h). For water strider's leg of strong superhydrophobicity and low water adhesion [8,9,30], the variation was not obvious, but the difference between the opposite directions was enough to be clearly distinguished. Hereby, the adhesion to water droplet dependent on direction was perceived and it was demonstrated that the orientation of the aligned setae affected water sliding.

Since the direction-dependent adhesion on water strider's leg was verified in rolling and sliding experiment, to quantitatively explore the interaction between water strider's leg and water, a measurement according to Wilhelmy method was utilized with the high-precision microelectronic balance (Fig. 4) [17,31]. This method enables force difference to be precise to 0.01 dyne, and is sufficient to detect the tiny force difference resulted from the setae orientation. A segment of water strider's leg, which is straight with a uniform diameter of $\sim 220 \mu\text{m}$ from the tip to end, is selected to suspend on the microelectronic balance vertically in a given orientation (AS or OS, illustrated in Fig. 4a). A water vessel placed below the leg is lifted to contact the leg at a constant velocity up to a given depth. Meanwhile, the variation of the measured force with the immersion depth is automatically recorded by the system. The force measured by the microelectronic balance can be described by the equation [16,17]: $F = F_w + F_g - F_b$, where F is the measured force, F_w is the wetting force, corresponding to the interaction between water and water strider's leg, F_g is the leg weight, initialized to zero before the leg contacts water surface, and F_b is the buoyancy force of the leg when it is immersed in water, which can be negligible, compared to F_w . Therefore, the wetting force (F_w) is approximately estimated by the measured force (F).

Fig. 4b shows the variation of the wetting force with the immersion depth when the leg is gradually immersed in water, along the OS or AS orientation. The negative force on the curves meant that the wetting force acted as a resistance when the leg is immersed in water. Owing to the surface roughness and heterogeneity of hairy strider leg, the measured curves in Fig. 4b aren't smooth but zigzag, and the average force in two different immersion directions can be analyzed. It was evident that during the immersion process, a larger wetting force (av. 2.5 ± 0.3 dyne) is measured in the OS direction than that in the AS direction (av. 0.7 ± 0.5 dyne). Thus the larger resistance existed when water strider's leg was immersed in water in the OS direction than in the AS direction. The wetting force was attributed to several

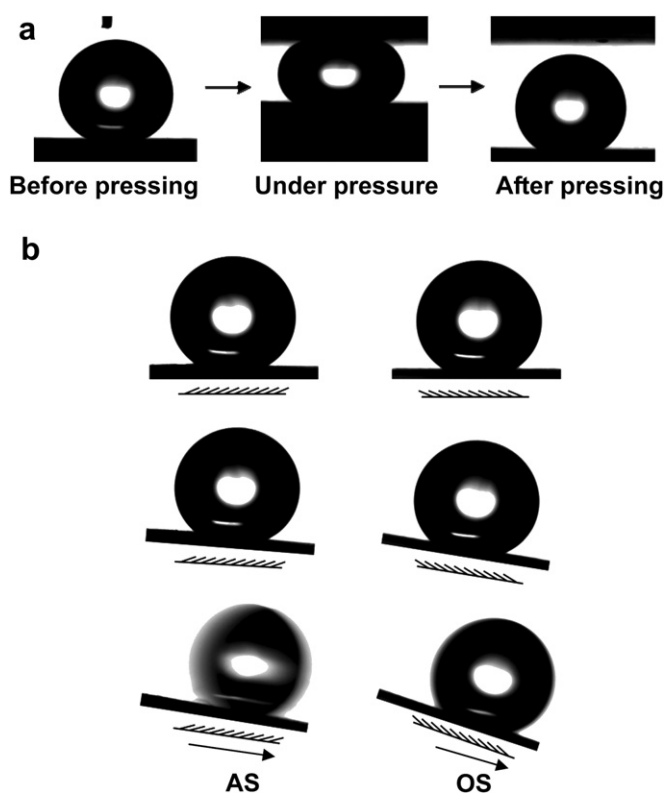


Fig. 2. Rolling behaviors of water droplet on the close-packed-leg surface of eight legs in the AS and OS direction. After water droplet is pressed (a), it inclines to roll off along surface in the AS direction obviously rather than in the OS direction (b).

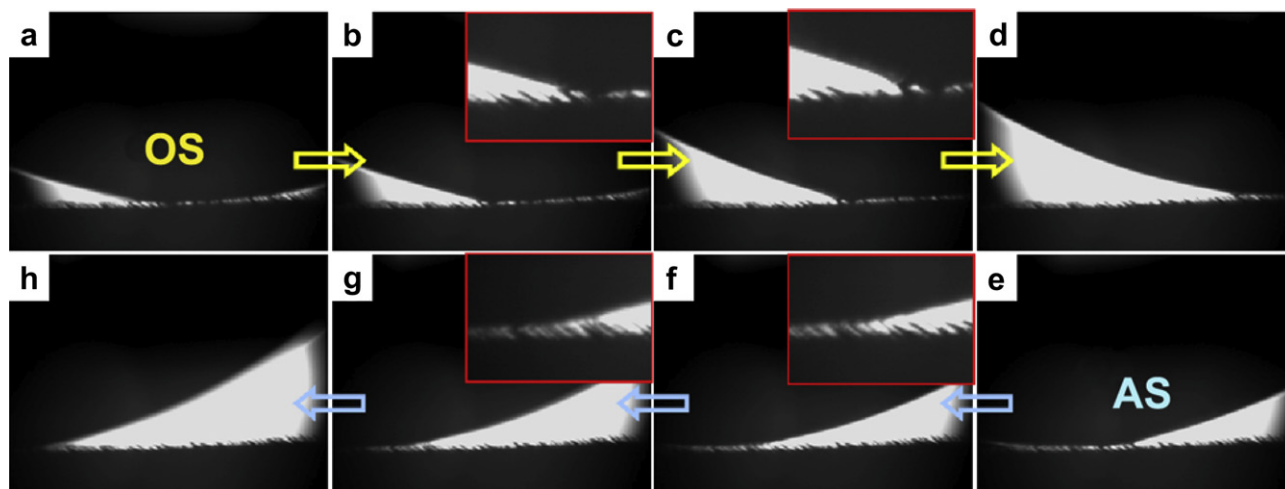


Fig. 3. Different adhesions exist in a water droplet sliding along a water strider's leg back and forth. The arrows denote the sliding direction of water droplet. (a)–(d) A water droplet slid in the OS direction. Some adhesion happened at interface of water and setae, accompanying relatively extending contact between water and setae, with continuous TCL. The setae increased its inclination angle (the insets of (b) and (c)). (e)–(h) A water droplet slid in the AS direction. The water droplet suspended onto setae, and clearly in a typical Cassie's mode, accompanying discontinuous TCL, meanwhile, the setae slightly decreased its inclination angle (the insets of (f) and (g)).

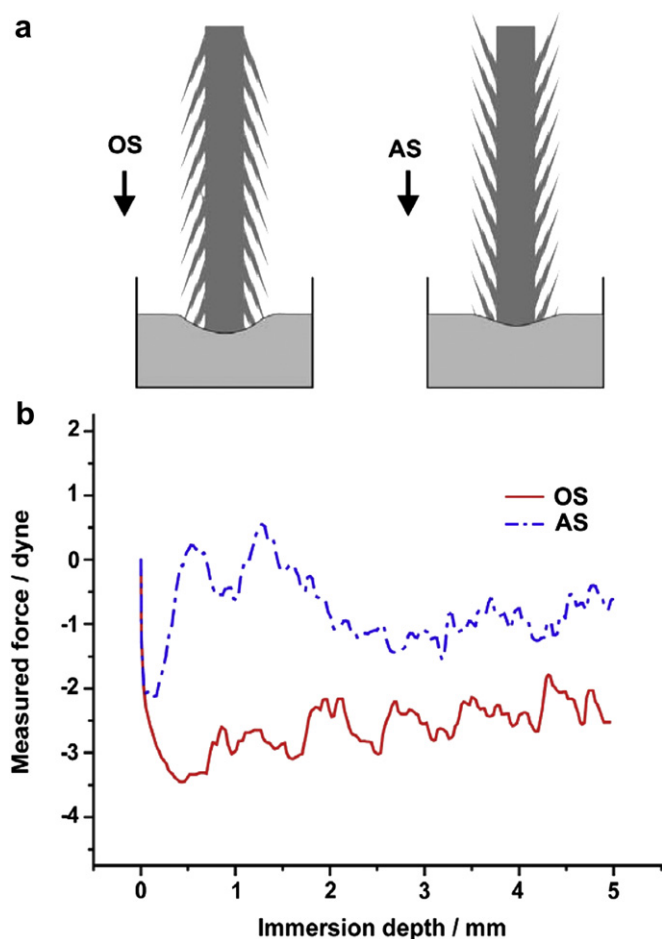


Fig. 4. Schematic and force curves of the interaction between water strider's leg and water droplet in the immersion experiments. (a) Schematic of the interaction between water strider's leg and water droplet in different directions (OS and AS). (b) The force curves of the interaction between water and leg in the two cases of (a). It is evident that when the sample is gradually immersed in water, larger wetting force exhibits in the OS direction than that in the AS direction.

factors such as surface chemical composition, roughness, surface deformability and heterogeneity, adsorption and desorption [16]. In this system, all the conditions of the measurement in two opposite setae orientation of leg were the same. Therefore, only the orientations of the setae can give rise to the difference in the wetting force.

In order to further clarify the effects of the setae orientation on directional adhesion of water strider's leg for water-walking propulsion, a model was proposed as shown in Fig. 5. In normal case, the setae arrays orientally align on surface of water strider's leg, with an inclination angle of θ to leg surface. Its unique hierarchical structures can involve an air cushion between water and leg for water repellency, where water would just contact tips of the setae but not penetrated into gaps among the setae (Fig. 5a). For the thoroughly discontinuous TCL and low adhesion, setae orientation could hardly affect the rolling behavior of water, which generates the unobvious directional rolling properties of water droplet on the close-packed-leg surface at one-dimensional level. When exerted an external pressure, water might partially penetrate the area cushion on the surface microstructure more or less and get into the gaps between setae (Fig. 5b). In this case, the contour, length and continuity of the TCL changed, which controlled the rolling or adhering of water droplet [26,27], so that distinct direction-dependent rolling properties were observed. The TCL got longer and less continuous, which could be pinned on side surface of setae, exerting an influence on the inclination of the setae. The flexibility of the setae on leg accompanying with the water repellency enables the inclination angle θ vary with the relatively moving direction between water strider's leg and water. When relative motion happened in the AS direction, the aligned setae tilted downwards to leg with θ decreasing to θ_1 (Fig. 5c), the TCL length decreased, and water could easily slide along the setae, thus a lower resistance or adhesion generates. As for relative motion in the OS direction, the aligned setae tilted upwards away from leg with θ increasing to θ_2 (Fig. 5d), the turnout setae could hamper this relative motion and extend the contact between water and setae, displaying a larger resistance or adhesion. Based on this model, it can be elucidated that the orientation of the aligned setae on leg affected adhesive behavior in water droplet rolling and sliding, and generates asymmetric water resistance during relative motion between leg and water, which exhibits direction-dependent adhesion of leg in the water-walking propulsion of water strider. This result might

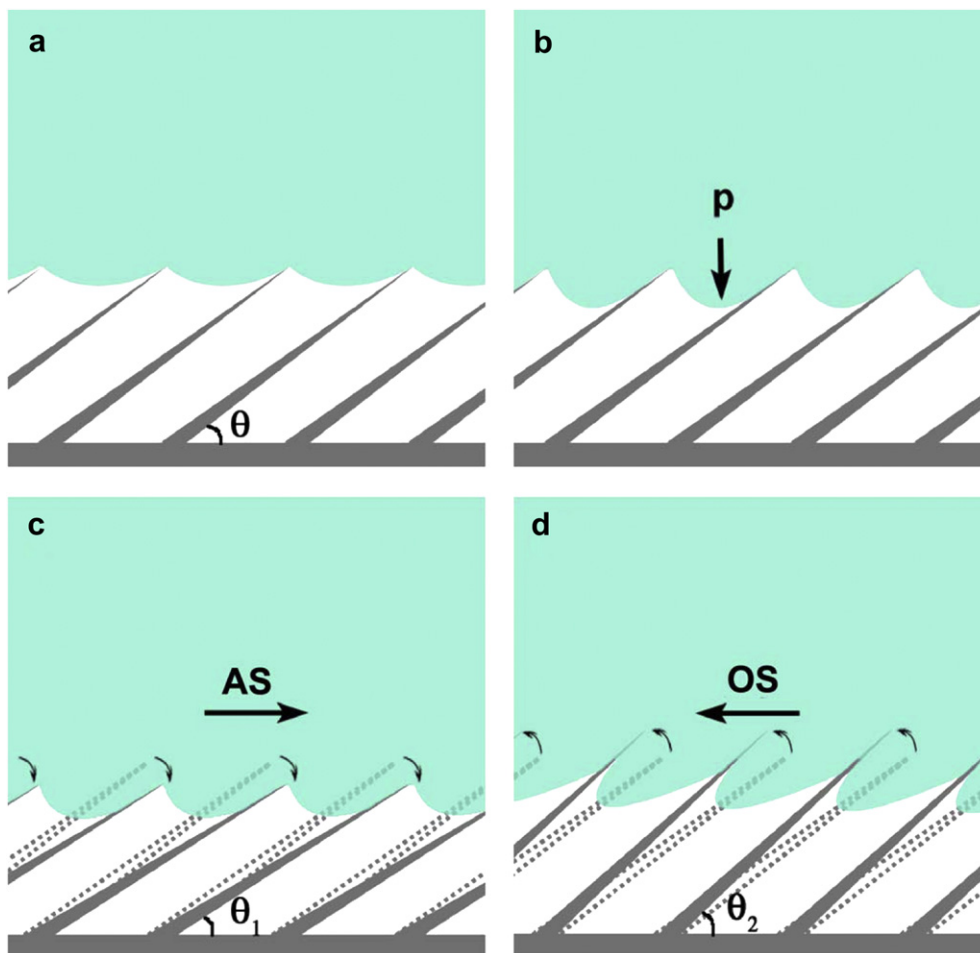


Fig. 5. Model that flexibly oriented setae on water strider's leg forms asymmetric adhesion for water-walking propulsion of water strider. (a) Water exists on the tips of the oriented setae without wetting side surface of the setae, and θ is the original inclination angle. (b) When a pressure p is applied, water may get into gaps among the setae and then the setae are partially wetted. (c) θ decreases to θ_1 when relative motion occurs between leg and water in the AS direction. (d) θ increases to θ_2 when relative motion happens between leg and water in the OS direction. The arrows denote the direction of relative motion between water and leg.

demonstrate the reason why a water strider stands on water surface, usually keeping a posture that let the aligned setae of its leg oppose water in the OS orientation. With the leg in this setae orientation, water striders are hard to drown in water due to the large resistance; on the other hand, even when their legs pierce the water surface in a violent torrent or storm, they can hardly drown down and easily float up due to the smaller resistance in the opposite direction. Therefore, the unique setae orientation could assist the water strider standing and walking on water surface effortlessly.

4. Conclusions

We revealed that direction-dependent adhesion of water strider's leg for water-walking propulsion of water strider is resulted from the orientally aligned setae. The flexibly oriented setae of water strider's legs tune effectively the solid–liquid–air three phase interface along two contrasting directions: the direction along the setae and opposite the setae when the water strider walks on water surface, accordingly, the unique asymmetric adhesion of water strider's leg is induced, which endowed water strider with smart abilities to stably stand and walk effortlessly on water surface. With the leg contacting water in a posture like the OS orientation, the water strider should be hard to drown in water, and easy to float up even when water strider's leg pierces water surface.

This finding offers an insight into the effect of oriented structure responsible for water-walking behavior of insect living on water, and inspires us to design novel structured surface that can be applied in microfluidic and aquatic devices.

Acknowledgments

This work is supported by National Research Fund for Fundamental Key Project (2010CB934700), National Natural Science Foundation of China (20973018), and Doctoral Fund of Ministry of Education of China (20101102110035, 20121102110035).

References

- [1] E. Bowdan, J. Comp. Physiol. 123 (1978) 43.
- [2] M. Dickinson, Nature 424 (2003) 621.
- [3] M.W. Denny, J. Exp. Biol. 207 (2004) 1601.
- [4] D.L. Hu, B. Chan, J.W.M. Bush, Nature 424 (2003) 663.
- [5] D.L. Hu, J.W.M. Bush, Nature 437 (2005) 733.
- [6] J.W.M. Bush, D.L. Hu, Annu. Rev. Fluid Mech. 38 (2006) 339.
- [7] J.W.M. Bush, D.L. Hu, M. Prakash, Adv. Insect Physiol. 34 (2008) 117.
- [8] X.F. Gao, L. Jiang, Nature 432 (2004) 36.
- [9] X.Q. Feng, X.F. Gao, Z.N. Wu, L. Jiang, Q.S. Zheng, Langmuir 23 (2007) 4892.
- [10] F. Shi, J. Niu, J.L. Liu, F. Liu, Z.Q. Wang, X.Q. Feng, X. Zhang, Adv. Mater. 19 (2007) 2257.
- [11] Y.S. Song, M. Sitti, IEEE Trans. Robot. 23 (2007) 578.
- [12] X.F. Wu, G.Q. Shi, J. Phys. Chem. B 110 (2006) 11247.
- [13] A.S. Ghasseminia, A. Faraji, J. Bionic Eng. 5 (2008) 87.

- [14] L. Feng, S.H. Li, Y.S. Li, H.J. Li, L.J. Zhang, J. Zhai, Y.L. Song, B.Q. Liu, L. Jiang, D.B. Zhu, *Adv. Mater.* 14 (2002) 1857.
- [15] Y.M. Zheng, X.F. Gao, L. Jiang, *Soft Matter* 3 (2007) 178.
- [16] R. Molina, F. Comelles, M.R. Julia, P. Erra, *J. Colloid Interface Sci.* 237 (2001) 40.
- [17] R.A. Lodge, B. Bhushan, *J. Appl. Polym. Sci.* 102 (2006) 5255.
- [18] R.J. Kennedy, *Nature* 227 (1970) 736.
- [19] M. Gleiche, L.F. Chi, H. Fuchs, *Nature* 403 (2000) 173.
- [20] Z. Yoshimitsu, A. Nakajima, T. Watanabe, K. Hashimoto, *Langmuir* 18 (2002) 5818.
- [21] R. Seemann, M. Brinkmann, E.J. Kramer, F.F. Lange, R. Lipowsky, *Proc. Natl. Acad. Sci. U. S. A.* 102 (2005) 1848.
- [22] J.Y. Chung, J.P. Youngblood, C.M. Stafford, *Soft Matter* 3 (2007) 1163.
- [23] D.Y. Xia, S.R.J. Brueck, *Nano Lett.* 8 (2008) 2819.
- [24] C.W. Extrand, *Langmuir* 23 (2007) 1867.
- [25] T.L. Sun, L. Feng, X.F. Gao, L. Jiang, *Acc. Chem. Res.* 38 (2005) 644.
- [26] T. Onda, S. Shibuichi, N. Satoh, K. Tsujii, *Langmuir* 12 (1996) 2125.
- [27] W. Chen, A.Y. Fadeev, M.C. Hsieh, D. Oner, J. Youngblood, T.J. McCarthy, *Langmuir* 15 (1999) 3395.
- [28] A. Lafuma, D. Quere, *Nat. Mater.* 2 (2003) 457.
- [29] C. Ishino, K. Okumura, D. Quere, *Europhys. Lett.* 68 (2004) 419.
- [30] P.J. Wei, S.C. Chen, J.F. Lin, *Langmuir* 25 (2009) 1526.
- [31] L. Wilhelmy, *Ann. Phys.* 6 (1863) 177.